Supplementary information
Similarity and Dynamic Characteristics of Triboelectric Nanogenerators

SI 1 : For *Dynamics model and similarity*

SI 1.1 Derivation of the dynamic model

The governing equation is

$$R\frac{\mathrm{d}Q}{\mathrm{d}t} = V_{OC} - \frac{Q}{C} \tag{S1}$$

Considering $Q_{SC} = V_{OC}C$, we have

$$\frac{1}{RC}Q + \frac{\mathrm{d}Q}{\mathrm{d}t} = \frac{1}{RC}Q_{SC} \tag{S2}$$

where the open circuit voltage V_{OC} and the capacitance C are functions of the ralative displacement x between the two electrodes. Nondimensionalize Eq.(S2) using the characteristic charge quantity q (which can be taken as the tribocharge quantity σWL), the characteristic time T (for periodic motion, the period can be used) and the characteristic capacitance C_0 (which can be taken as the capacitance of the parallel-plate capacitor formed by triboelectric layers at the initial position)

$$\frac{T}{RC_0}\frac{1}{\frac{C}{C_0}}\frac{Q}{q} + \frac{\mathrm{d}\frac{Q}{q}}{\mathrm{d}\frac{t}{T}} = \frac{T}{RC_0}\frac{1}{\frac{C}{C_0}}\frac{Q_{SC}}{q} \tag{S3}$$

Let $\hat{Q} = \frac{Q}{q}$, $\hat{j} = \frac{Q_{SC}}{q}$, $\hat{g}^{-1} = \frac{C}{C_0}$ and $\hat{t} = \frac{t}{T}$, representing the dimensionless transferred charge quantity, the dimensionless SC transferred charge quantity, the dimensionless capacitance and the dimensionless time, respectively. We have

$$\frac{1}{S_m}\frac{\mathrm{d}\hat{Q}}{\mathrm{d}\hat{t}} + \hat{g}\hat{Q} = \hat{g}\hat{j} \tag{S4}$$

where $S_m = \omega_0 T = \frac{T}{RC_0}$. Its solution is

$$\hat{Q}(\hat{t}) = \frac{1}{\hat{K}}\int \hat{j}\mathrm{d}\hat{K} \tag{S5}$$

where $\hat{K} = e^{S_m\hat{G}} = e^{S_m\int \hat{g}\mathrm{d}\hat{t}}$. According to Eq.(S4), the current I can be expressed as

$$I = \frac{\mathrm{d}Q}{\mathrm{d}t} = \frac{q}{T}\frac{\mathrm{d}\hat{Q}}{\mathrm{d}\hat{t}} = \omega_0 q\hat{g}(\hat{j} - \hat{Q}) \tag{S6}$$

The electrostatic force F, generated during the movement of the TENG, can be obtained in the following way. The voltage across the electrodes is

$$V = -\frac{Q}{C} + V_{OC} \tag{S7}$$

the electrostatic energy of transferred charges is

$$U_{e1} = -\int V\mathrm{d}Q = \frac{1}{2}\frac{1}{C}Q^2 - V_{OC}Q \tag{S8}$$

And the electrostatic energy of tribocharges is

$$U_{e2} = \frac{1}{2}V_{OC}q \tag{S9}$$

Therefore the total electrostatic energy of the TENG is

$$U_e = U_{e1} + U_{e2} = \frac{1}{2} ARq^2 \hat{g} \left(\hat{Q}^2 - 2\hat{j}\hat{Q} + \hat{j} \right) \tag{S10}$$

Denote the relative motion of the TENG as $x(t) = Df(t)$, D being the characteristic length. Assuming that the work done to overcome the electrostatic force F causes a change in the electrostatic energy on the one hand, and is consumed by the resistor of the external circuit on the other, it is easy to obtain

$$-F\frac{\mathrm{d}x}{\mathrm{d}t} = \frac{\mathrm{d}U_e}{\mathrm{d}t} + I^2 R \tag{S11}$$

Then we have

$$\begin{aligned} F &= -\frac{1}{2D}\omega_0 Rq^2 \left(\frac{\hat{g}'}{\hat{x}'}\hat{Q}^2 + \frac{(\hat{g}\hat{j})'}{\hat{x}'}(1 - 2\hat{Q}) \right) \\ &= -\frac{1}{2D}\omega_0 Rq^2 \left(\frac{\mathrm{d}\hat{g}}{\mathrm{d}\hat{x}}\hat{Q}^2 + \frac{\mathrm{d}(\hat{g}\hat{j})}{\mathrm{d}\hat{x}}(1 - 2\hat{Q}) \right) \end{aligned} \tag{S12}$$

In the case of the examined lateral sliding mode TENG, we have

$$C_0 = \frac{\epsilon_0 WL}{\delta} \tag{S13}$$

$$C = \frac{\epsilon_0 W(L - x)}{\delta} \tag{S14}$$

$$Q_{SC} = \sigma x W \tag{S15}$$

where $\delta = \epsilon_0 d_1/\epsilon_1 + \epsilon_0 d_2/\epsilon_2$ is the effictive thicknesses. Then

$$\omega_0 = \frac{1}{RC_0} = \frac{\delta}{\epsilon_0 WLR} \tag{S16}$$

$$\hat{g} = \frac{C_0}{C} = \frac{1}{1 - \frac{x}{L}} = \frac{1}{1 - \hat{x}} \tag{S17}$$

$$\hat{j} = \frac{Q_{SC}}{q} = \frac{\sigma x W}{\sigma WL} = \hat{x} \tag{S18}$$

Therefore

$$I = \frac{\delta\sigma}{\epsilon_0 R}\frac{\hat{x} - \hat{Q}}{1 - \hat{x}} \tag{S19}$$

$$F = -\frac{\delta\sigma^2 W}{2\epsilon_0}\frac{\left(1 - \hat{Q}\right)^2}{(1 - \hat{x})^2} \tag{S20}$$

Moreover, based on these discussions, we can present a numerical method for computing the dynamical response of TENGs under arbitrary motion inputs.

$$\hat{Q}_n = \frac{1}{\hat{K}_n}\sum_{i=1}^{n} \hat{j}_i \Delta\hat{K}_i \tag{S21}$$

$$\hat{K}_i = e^{S_m \hat{G}_i} \tag{S22}$$

$$\hat{G}_i = \sum_{l=1}^{i} \hat{g}_l \Delta\hat{t}_l \tag{S23}$$

$$\hat{Q}_0 = \hat{Q}(0) = 0, \hat{K}_0 = \hat{K}(0) = 1, \hat{G}_0 = \hat{G}(0) = 0 \tag{S24}$$

SI 1.2 Verification

The numerical method is validated by comparing its results with simulation data from the finite element analysis software COMSOL Multiphysics under three different motion input functions. The parameters of the tested TENG are shown Tab.(S1).

Table S1: Parameters of the tested lateral sliding mode TENG.

Parameter	Value
L	20mm
W	1000mm
d_1	0.2mm
d_2	0.2mm
ϵ_1/ϵ_0	4
ϵ_2/ϵ_0	2
R	$2\times10^8\Omega$
σ	$10^{-6}\mathrm{C/m^2}$

The three tested motion inputs are

$$x(t)=\begin{cases}8\left(1-\cos\left(4\pi t\right)\right), & N\le t\le N+\frac{1}{2}\\ 0, & N+\frac{1}{2}<t\le N+1\end{cases} \tag{S25}$$

$$x(t)=\begin{cases}64t, & N\le t\le N+\frac{1}{4}\\ 32-64t, & N+\frac{1}{4}\le t\le N+\frac{1}{2}\\ 0, & N+\frac{1}{2}<t\le N+1\end{cases} \tag{S26}$$

$$x(t)=\begin{cases}8\left(1-\cos\left(12\pi t\right)\right), & N\le t\le N+\frac{1}{6}\\ 0, & N+\frac{1}{6}<t\le N+1\end{cases} \tag{S27}$$

where N is a non-negative integer. The three motion inputs, along with the corresponding TENG current output and electrostatic force, are illustrated in Fig.(S1), Fig.(S2) and Fig.(S3), respectively.

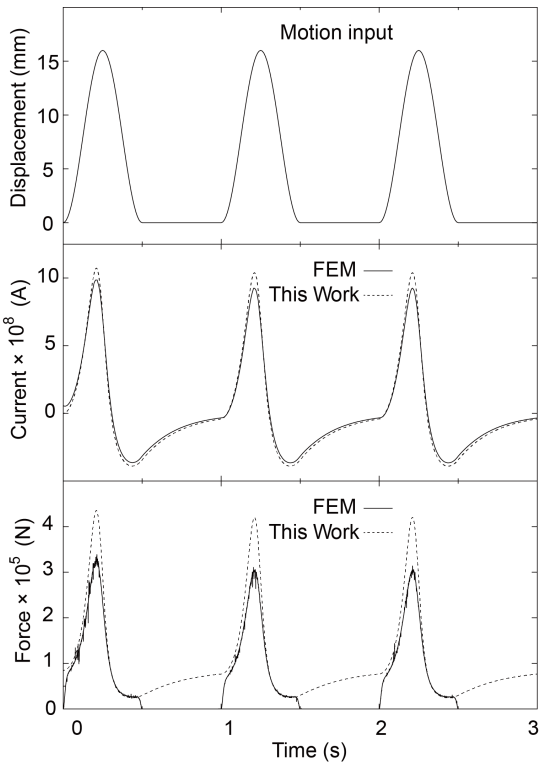

Figure S1: The motion input expressed in Eq.(S25) along with the corresponding TENG current output and electrostatic force from the dynamics model and the FEM simulation.

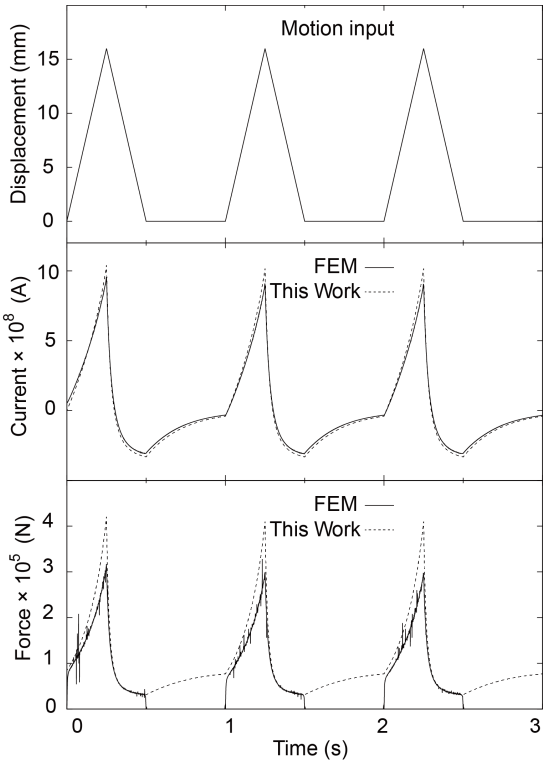

Figure S2: The motion input expressed in Eq.(S26) along with the corresponding TENG current output and electrostatic force from the dynamics model and the FEM simulation.

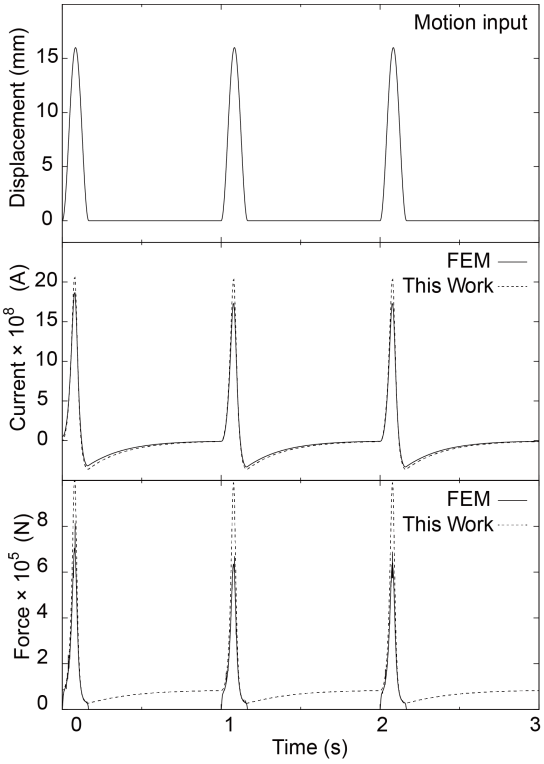

Figure S3: The motion input expressed in Eq.(S27) along with the corresponding TENG current output and electrostatic force from the dynamics model and the FEM simulation.

Note that Eq.(S12) implicitly assumes $\hat{x}' \neq 0$, therefore the calculation of electrostatic force is not applicable when $\hat{x}' = 0$, and this is also reflected in Fig.(S2) and Fig.(S3), but it does not significantly affect the qualitative description and analysis of electrostatic force. Overall, under various motion inputs, the dynamics model agrees well with the FEM simulation, largely demonstrating its validity.

SI 1.3 Similarity of EMGs

The EMG with a structure analogous to the lateral sliding TENG is shown in Fig.(S4). The EMG possesses the same principal dimensions as the TENG, with the length and width of its magnets and rectangular coil also denoted as L and W, respectively. The magnetic flux density is denoted as B. The external load is characterized by a simple pure resistive circuit, with the resistance denoted as R_E. The displacement of the coil is denoted by x.

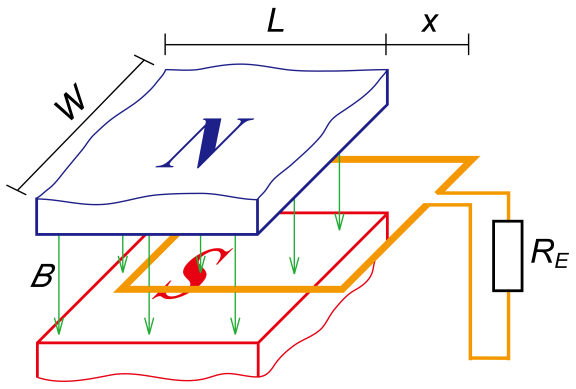

Figure S4: Schematic of the structures of the EMG.

The governing equation is

$$I = -\frac{1}{R_E}\frac{\mathrm{d}\phi}{\mathrm{d}t} \tag{S28}$$

Nondimensionalize Eq.(S28) using the characteristic magnetic flux BWL and the characteristic time T (for periodic motion, the period can be used)

$$\hat{I} = \frac{I}{\frac{BWL}{R_E T}} = -\frac{\mathrm{d}\hat{\phi}}{\mathrm{d}\hat{t}} \tag{S29}$$

Eq.S29 is devoid of any similarity criteria, indicating that the EMG operation process is unconditionally similar. Consequently, provided that two EMGs possess geometrically similar structures and analogous input motion curves, their respective currents, power outputs, and electromagnetic forces can be interconverted through a simple proportionality factor. In the case of the EMG illustrated in Fig.S4, we have

$$I = \frac{BWL}{R_E T}\frac{\mathrm{d}\hat{x}}{\mathrm{d}\hat{t}} \tag{S30}$$

$$F = -\frac{B^2W^2L}{R_E T}\frac{\mathrm{d}\hat{x}}{\mathrm{d}\hat{t}} \tag{S31}$$

SI 2 : For *Periodicity*

We have

$$\hat{x}\left(\hat{t}+1\right) = \hat{x}\left(\hat{t}\right) \tag{S32}$$

In general, the capacitance C and the short circuit transfer charge Q_{SC} are simple functions of the dimensionless displacement $\hat{x}$, so we have

$$\hat{g}\left(\hat{t}+1\right) = \hat{g}\left(\hat{t}\right) \tag{S33}$$

$$\hat{j}\left(\hat{t}+1\right) = \hat{j}\left(\hat{t}\right) \tag{S34}$$

then

$$\hat{G}\left(\hat{t}+1\right) = \int_0^{\hat{t}+1}\hat{g}\mathrm{d}u = \left(\int_0^1 + \int_1^{\hat{t}+1}\right)\hat{g}\mathrm{d}u = \hat{G}(1) + \hat{G}\left(\hat{t}\right) \tag{S35}$$

$$\hat{K}\left(\hat{t}+1\right) = e^{S_m\hat{G}\left(\hat{t}+1\right)} = e^{S_m\hat{G}(1)}e^{S_m\hat{G}\left(\hat{t}\right)} = \hat{K}(1)\hat{K}\left(\hat{t}\right) \tag{S36}$$

Therefore, for $\hat{t} = N + \hat{\xi}$, where $0 \le \hat{\xi} < 1$ and N is a non-negative integerit, is easy to get

$$\hat{g}\left(\hat{t}\right) = \hat{g}\left(\hat{\xi}\right) \tag{S37}$$

$$\hat{j}\left(\hat{t}\right) = \hat{j}\left(\hat{\xi}\right) \tag{S38}$$

$$\hat{G}\left(\hat{t}\right) = N\hat{G}(1) + \hat{G}\left(\hat{\xi}\right) \tag{S39}$$

$$\hat{K}\left(\hat{t}\right) = \hat{K}^N(1)\hat{K}\left(\hat{\xi}\right) \tag{S40}$$

Considering $\mathrm{d}\hat{K} = S_m\hat{g}\hat{K}\mathrm{d}\hat{t}$, we have

$$\hat{Q}\left(\hat{t}\right) = \frac{1}{\hat{K}\left(\hat{t}\right)}\int_{\hat{K}(0)}^{\hat{K}\left(\hat{t}\right)}\hat{j}\mathrm{d}\hat{K} = \frac{1}{\hat{K}\left(\hat{t}\right)}\int_0^{\hat{t}} S_m\hat{g}\hat{j}\hat{K}\mathrm{d}u = \frac{1}{\hat{K}\left(\hat{t}\right)}\int_0^{\hat{t}} p\mathrm{d}u \tag{S41}$$

where $p = S_m\hat{g}\hat{j}\hat{K}$. Obviously

$$p\left(\hat{t}\right) = \hat{K}^N(1)p\left(\hat{\xi}\right) \tag{S42}$$

then

$$\begin{aligned}\hat{Q}\left(\hat{t}\right) &= \frac{1}{\hat{K}^N(1)\hat{K}\left(\hat{\xi}\right)}\left(\int_0^1+\int_1^2+...+\int_{N-1}^N+\int_N^{N+\hat{\xi}}\right)p\mathrm{d}u \\ &= \frac{1}{\hat{K}^N(1)\hat{K}\left(\hat{\xi}\right)}\left(\left(1+\hat{K}(1)+...+\hat{K}^{N-1}(1)\right)\int_0^1 p\mathrm{d}u+\hat{K}^N(1)\int_0^{\hat{\xi}}p\mathrm{d}u\right) \\ &= \frac{1}{\hat{K}^N(1)\hat{K}\left(\hat{\xi}\right)}\left(\frac{\hat{K}^N(1)-1}{\hat{K}(1)-1}\int_0^1 p\mathrm{d}u+\hat{K}^N(1)\int_0^{\hat{\xi}}p\mathrm{d}u\right) \\ &= \hat{Q}(1)\frac{1-\hat{K}^{-N}(1)}{1-\hat{K}^{-1}(1)}\frac{1}{\hat{K}\left(\hat{\xi}\right)}+\hat{Q}\left(\hat{\xi}\right)\end{aligned} \tag{S43}$$

SI 3 : For *Limiting conditions*

As $S_m \to 0$

$$\hat{K}_{S_m\to 0} = e^{S_m\hat{G}}|_{S_m\to 0} = 1+S_m\hat{G}+o\left(S_m^2\right) \tag{S44}$$

$$\hat{Q}_{S_m\to 0} = S_m\frac{1}{\hat{K}_{S_m\to 0}}\int_0^{\hat{t}}\hat{j}\hat{g}\hat{K}_{S_m\to 0}\mathrm{d}\hat{t} = S_m\int_0^{\hat{t}}\hat{j}\hat{g}\mathrm{d}\hat{t} \tag{S45}$$

$$\begin{aligned}\hat{Q}^S_{S_m\to 0}\left(\hat{t}\right) &= \hat{Q}_{S_m\to 0}(1)\frac{1}{1-\hat{K}^{-1}_{S_m\to 0}(1)}\frac{1}{\hat{K}_{S_m\to 0}\left(\hat{t}\right)}+\hat{Q}_{S_m\to 0}\left(\hat{t}\right) \\ &= \frac{\int_0^1\hat{j}\hat{g}\mathrm{d}\hat{t}}{\int_0^1\hat{g}\mathrm{d}\hat{t}}\frac{1+S_m\int_0^1\hat{g}\mathrm{d}\hat{t}}{1+S_m\int_0^{\hat{t}}\hat{g}\mathrm{d}\hat{t}}+S_m\int_0^{\hat{t}}\hat{j}\hat{g}\mathrm{d}\hat{t} \\ &= \frac{\int_0^1\hat{j}\hat{g}\mathrm{d}\hat{t}}{\int_0^1\hat{g}\mathrm{d}\hat{t}}\end{aligned} \tag{S46}$$

Considering the relationship $\hat{g}\hat{j} = \hat{g}-1$ inherent to the lateral sliding mode TENG, we have

$$\hat{Q}^S_{S_m\to 0} = \frac{\int_0^1\hat{j}\hat{g}\mathrm{d}\hat{t}}{\int_0^1\hat{g}\mathrm{d}\hat{t}} = 1-\frac{1}{\int_0^1\hat{g}\mathrm{d}\hat{t}} = 1-\frac{1}{\hat{G}(1)} \tag{S47}$$

where $\hat{G}(1) = \int_0^1\hat{g}\mathrm{d}\hat{t}$.

SI 4 : For *Optimal motion input*

SI 4.1 Optimal shape function

First assume that the shape function $\hat{x}$ varies within the range $[0,\hat{x}_m]$. Since $\hat{g}$ increases monotonically with $\hat{x}$, $\hat{g}$ takes values in $[1,\hat{g}_m]$, where $\hat{g}_m = \hat{g}|_{\hat{x}=\hat{x}_m}$. At this point, the problem can be transformed into finding the function $\hat{g}_{opt}(\hat{t})$ with a domain of $[0,1]$ and a range of $[1,\hat{g}_m]$, such that the average power output $\overline{P^S_{T\to 0}}$ is maximized.

The average power output is

$$\overline{P^S_{T\to 0}} = \lim_{T\to 0}\left(\frac{1}{T}\int_0^T\left(I^S(t)\right)^2R\mathrm{d}t\right) = R\int_0^1\left(I^S_{T\to 0}(\hat{t})\right)^2\mathrm{d}\hat{t} = \omega_0^2q^2R\int_0^1\left(\frac{\hat{g}}{\hat{G}(1)}-1\right)^2\mathrm{d}\hat{t} \tag{S48}$$

Observe the following integral S

$$S = \int_0^1\left(\frac{\hat{g}}{\hat{G}(1)}-1\right)^2\mathrm{d}\hat{t} \tag{S49}$$

It can actually be seen as the variance of the set formed by discretizing the function $\frac{\hat{g}}{\hat{G}(1)}$, and the reason is briefly described as follows. First, $\hat{t} \in (0,1)$ is uniformly discretized into $\{\hat{t}_1, ..., \hat{t}_N\}$, denoted as $\{\hat{t}_i\}$, and the corresponding function values are discretized into $\{\hat{g}_1, ..., \hat{g}_N\}$, denoted as $\{\hat{g}_i\}$. Then, as shown in Fig.(S5), $G(1)$ can be viewed as the average value $\overline{\hat{g}}$ of $\{\hat{g}_i\}$.

$$\hat{G}(1) = \int_0^1 \hat{g} \mathrm{d}\hat{t} = \lim_{N\to\infty} \frac{1}{N} \sum_{i=1}^{N} \hat{g}_i = \overline{\hat{g}} \tag{S50}$$

Similarly, the integral $\int_0^1 \frac{\hat{g}}{\hat{G}(1)} \mathrm{d}\hat{t}$ can also be viewed as the average value $\overline{\left(\frac{\hat{g}}{\hat{G}(1)}\right)}$ of $\left\{\frac{\hat{g}_i}{\hat{G}(1)}\right\}$, and it happens to 1.

$$\overline{\left(\frac{\hat{g}}{\hat{G}(1)}\right)} = \int_0^1 \frac{\hat{g}}{\hat{G}(1)} \mathrm{d}\hat{t} = \frac{1}{\hat{G}(1)} \int_0^1 \hat{g} \mathrm{d}\hat{t} = 1 \tag{S51}$$

Therefore

$$S = \int_0^1 \left(\frac{\hat{g}}{\hat{G}(1)} - 1\right)^2 \mathrm{d}\hat{t} = \int_0^1 \left(\frac{\hat{g}}{\hat{G}(1)} - \overline{\left(\frac{\hat{g}}{\hat{G}(1)}\right)}\right)^2 \mathrm{d}\hat{t} = \lim_{N\to\infty} \frac{1}{N} \sum_{i=1}^{N} \left(\frac{\hat{g}_i}{\hat{G}(1)} - \overline{\left(\frac{\hat{g}}{\hat{G}(1)}\right)}\right)^2 \tag{S52}$$

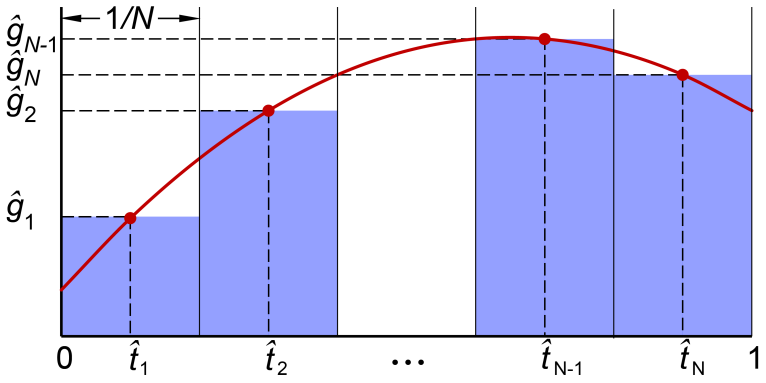

Figure S5: Discretization of $\hat{g}$.

S can be viewed as the variance of $\left\{\frac{\hat{g}_i}{\hat{G}(1)}\right\}$, which means: 1) the function values can be shuffled, that is, the function value sequence $\{\hat{g}_i\}$ and the independent variable sequence $\{\hat{t}_i\}$ can be one-to-one corresponded in any way while keeping the final integral value S unchanged; 2) the function g should be discretized as much as possible. Corollary 1 allows us to rearrange $\{\hat{g}_i\}$, so without loss of generality, it is assumed that the function $\hat{g}$ descreases with $\hat{t}$. Corollary 2 suggests that $\hat{g}$ should only take the value 1 or the maximum value $\hat{g}_m$. In conclusion, let

$$\hat{g} = \begin{cases} \hat{g}_m, & 0 \le \hat{t} \le a \\ 1, & a < \hat{t} \le 1 \end{cases} \tag{S53}$$

Substitute Eq.(S53) into Eq.(S49).

$$S = (\hat{g}_m - 1)^2 \left(a - a^2\right) \left((\hat{g}_m - 1)\, a + 1\right)^{-2} \tag{S54}$$

Let

$$\frac{\mathrm{d}S}{\mathrm{d}a} = 0 \tag{S55}$$

We can get

$$a = \frac{1}{\hat{g}_m + 1} \tag{S56}$$

Therefore, we obtain the optimal function $\hat{g}$-$\hat{t}$ under the limiting condition.

$$\hat{g}_{opt}(\hat{t}) = \begin{cases} \hat{g}_m, & 0 \le \hat{t} \le \frac{1}{\hat{g}_m+1} \\ 1, & \frac{1}{\hat{g}_m+1} < \hat{t} \le 1 \end{cases} \tag{S57}$$

Its corresponding shape function is

$$\hat{x}_{opt}(\hat{t}) = \begin{cases} \hat{x}_m, & 0 \le \hat{t} \le \frac{1}{\hat{g}_m+1} \\ 0, & \frac{1}{\hat{g}_m+1} < \hat{t} \le 1 \end{cases} \tag{S58}$$

SI 4.2 Verification by numerical means

When $\hat{x}_m = 0.8$, the optimal shape function is

$$\hat{x}_{opt}\left(\hat{t}\right) = \begin{cases} 0.8, & 0 \le \hat{t} \le \frac{1}{6} \\ 0 & \frac{1}{6} < \hat{t} \le 1 \end{cases} \tag{S59}$$

For the sake of prudence, we also utilized numerical methods to calculate the optimal shape function.

Found a function $\hat{x}$ defined on $[0,1]$ with range $[0,\hat{x}_m]$ such that the integral S attains its maximum value.

$$S = \int_0^1 \left(\frac{\hat{g}}{\hat{G}(1)} - 1\right)^2 \mathrm{d}\hat{t} \tag{S60}$$

where $\hat{g} = 1/(1-\hat{x})$ for lateral sliding mode TENGs. Assuming that $\hat{x}$ is decreasing, $\hat{x}(0) = \hat{x}_m$ and $\hat{x}(1) = 0$. First, $\hat{t} \in [0,1]$ is uniformly discretized into $\{\hat{t}_i\} = \left\{\hat{t}_0 = 0, \hat{t}_1 = \frac{1}{N}, ..., \hat{t}_{N-1} = \frac{N-1}{N}, \hat{t}_N = 1\right\}$, and the corresponding function values are discretized into $\{\hat{x}_i\} = \{\hat{x}_0 = 0.8, \hat{x}_1, ..., \hat{x}_{N-1}, \hat{x}_N = 0\}$. At this point, $G(1)$ can be expressed as a limit sum form using $\{\hat{x}_i\}$.

$$\hat{G}(1) = \lim_{N\to\infty} \frac{1}{N} \sum_{i=1}^{N} \left(\frac{\hat{g}_i + \hat{g}_{i-1}}{2}\right) \tag{S61}$$

Let

$$z = \left(\frac{\hat{g}}{\hat{G}(1)} - 1\right)^2 \tag{S62}$$

then, $\{z_i\} = \left\{\left(\frac{\hat{g}_i}{\hat{G}(1)} - 1\right)^2\right\}$. Therefore

$$S = \int_0^1 z \mathrm{d}\hat{t} = \lim_{N\to\infty} \frac{1}{N} \sum_{i=1}^{N} \frac{z_i + z_{i-1}}{2} \tag{S63}$$

This can be viewed as a multi-parameter optimization problem with the objective function S and $N-1$ unknown parameters $\hat{x}_1, ..., \hat{x}_{N-1}$, subject to the constraint equations $\hat{x}_i > \hat{x}_{i+1} (1 \le i \le N-2), 0 \le \hat{x}_i \le \hat{x}_m (1 \le i \le N-1)$.

Using the differential evolution method to solve this problem, the Python library scikit-opt can easily call this algorithm. Let $N = 48$, set the initial population size to 5000, and set the iteration number to 100000. The numerical results are shown in Tab.(S2) and Fig.(S6), which are consistent with Eq.(S58).

Table S2: Numerical results of the optimal shape function.

$\hat{t}$	f	$\hat{t}$	f	$\hat{t}$	f
0	0.8	0.3542	7.5351E − 14	0.7083	1.4770E − 14
0.0208	8.0000E − 01	0.3750	6.3038E − 14	0.7292	1.3397E − 14
0.0417	8.0000E − 01	0.3958	6.2825E − 14	0.7500	9.3196E − 15
0.0625	8.0000E − 01	0.4167	6.1772E − 14	0.7708	7.6292E − 15
0.0833	8.0000E − 01	0.4375	4.8482E − 14	0.7917	4.2471E − 15
0.1042	8.0000E − 01	0.4583	4.8450E − 14	0.8125	4.2351E − 15
0.1250	8.0000E − 01	0.4792	4.8009E − 14	0.8333	4.0866E − 15
0.1458	8.0000E − 01	0.5000	4.7315E − 14	0.8542	3.8672E − 15
0.1667	8.0000E − 01	0.5208	4.6616E − 14	0.8750	3.6156E − 15
0.1875	1.0769E − 13	0.5417	3.3580E − 14	0.8958	3.3402E − 15
0.2083	1.0686E − 13	0.5625	3.3528E − 14	0.9167	2.3325E − 15
0.2292	1.0344E − 13	0.5833	3.2637E − 14	0.9375	2.1117E − 15
0.2500	9.2068E − 14	0.6042	3.2175E − 14	0.9583	8.5767E − 16
0.2708	9.0463E − 14	0.6250	1.8660E − 14	0.9792	4.7161E − 16
0.2917	8.9505E − 14	0.6458	1.8509E − 14	1	0
0.3125	7.7754E − 14	0.6667	1.7986E − 14		
0.3333	7.7651E − 14	0.6875	1.7194E − 14		

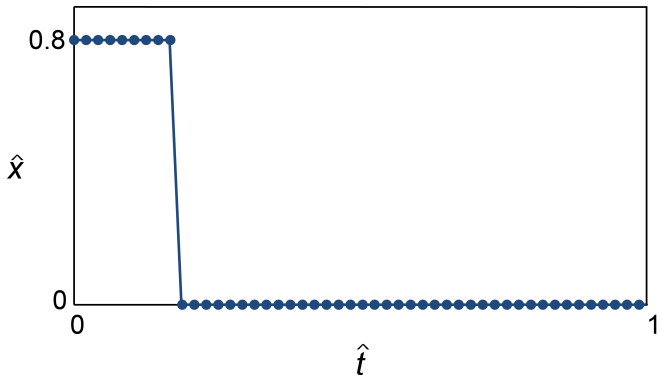

Figure S6: Numerical results of the optimal shape function.

SI 4.3 Optimal shape functions of the two composite motion inputs x_{opt}^{Har} and x_{opt}^{Tri}

The combination of harmonic wave and constant function is

$$\hat{x}\left(\hat{t}\right)=\begin{cases}\frac{\hat{x}_m}{2}\left(1-\cos\left(2\pi\omega\hat{t}\right)\right), & 0\leq\hat{t}\leq\frac{1}{\omega}\\ 0, & \frac{1}{\omega}<\hat{t}\leq 1\end{cases} \tag{S64}$$

Then

$$\hat{g}\left(\hat{t}\right)=\frac{1}{1-\hat{x}\left(\hat{t}\right)}=\begin{cases}\frac{1}{1-\frac{\hat{x}_m}{2}+\frac{\hat{x}_m}{2}\cos\left(2\pi\omega\hat{t}\right)}, & 0\leq\hat{t}\leq\frac{1}{\omega}\\ 1, & \frac{1}{\omega}<\hat{t}\leq 1\end{cases} \tag{S65}$$

Let the variable ω be adjusted such that the average power attains its maximum value, i.e.,

$$\frac{\mathrm{d}}{\mathrm{d}\omega}\int_0^1\left(\frac{\hat{g}}{\hat{G}(1)}-1\right)^2\mathrm{d}\hat{t}=\frac{\mathrm{d}}{\mathrm{d}\omega}\left(\omega\frac{\left(\frac{1}{2}\frac{2-\hat{x}_m}{(1-\hat{x}_m)^{\frac{3}{2}}}-1\right)+\omega}{\left(\left(\frac{1}{(1-\hat{x}_m)^{\frac{1}{2}}}-1\right)+\omega\right)^2}-1\right)=0 \tag{S66}$$

We get

$$\omega=\frac{4-4\sqrt{1-\hat{x}_m}-5\hat{x}_m+3\hat{x}_m\sqrt{1-\hat{x}_m}+2\hat{x}_m^2}{2-2\sqrt{1-\hat{x}_m}-4\hat{x}_m+3\hat{x}_m\sqrt{1-\hat{x}_m}+2\hat{x}_m^2}=\frac{4}{3}+\frac{5}{18}\hat{x}_m+\frac{53}{216}\hat{x}_m^2+\frac{289}{1296}\hat{x}_m^3+o(\hat{x}_m^4) \tag{S67}$$

The combination of triangular wave and constant function is

$$\hat{x}(\hat{t})=\begin{cases}k\hat{t}, & 0\le\hat{t}\le\frac{\hat{x}_m}{k}\\ 2\hat{x}_m-k\hat{t}, & \frac{\hat{x}_m}{k}<\hat{t}\le\frac{2\hat{x}_m}{k}\\ 0, & \frac{2\hat{x}_m}{k}<\hat{t}\le 1\end{cases} \tag{S68}$$

Then

$$\hat{g}(\hat{t})=\frac{1}{1-\hat{x}(\hat{t})}=\begin{cases}\frac{1}{1-k\hat{t}}, & 0\le\hat{t}\le\frac{\hat{x}_m}{k}\\ \frac{1}{1+k\hat{t}-2\hat{x}_m}, & \frac{\hat{x}_m}{k}<\hat{t}\le\frac{2\hat{x}_m}{k}\\ 1, & \frac{2\hat{x}_m}{k}<\hat{t}\le 1\end{cases} \tag{S69}$$

Let the variable k be adjusted such that the average power attains its maximum value, i.e.,

$$\frac{\mathrm{d}}{\mathrm{d}k}\int_0^1\left(\frac{\hat{g}}{\hat{G}(1)}-1\right)^2\mathrm{d}\hat{t}=\frac{\mathrm{d}}{\mathrm{d}k}\left(\frac{\frac{2}{k}\frac{\hat{x}_m^2}{1-\hat{x}_m}+1}{\left(-\frac{2}{k}\left(\ln\left(1-\hat{x}_m\right)+\hat{x}_m\right)+1\right)^2}-1\right)=0 \tag{S70}$$

We get

$$k=-\frac{2\hat{x}_m^2(\hat{x}_m+\ln(1-\hat{x}_m))}{1-(1-\hat{x}_m)^2+2(1-\hat{x}_m)\ln(1-\hat{x}_m)}=3\hat{x}_m+\frac{1}{2}\hat{x}_m^2+\frac{7}{20}\hat{x}_m^3+o(\hat{x}_m^4) \tag{S71}$$

SI 4.4 The tested case in Fig.3

Parameters of the tested TENG are shown in Tab.(S3)

Table S3: Parameters of the tested TENG.

Parameter	Value
L	20mm
W	20mm
d_1	0.2mm
d_2	0.2mm
ϵ_1/ϵ_0	4
ϵ_2/ϵ_0	2
R	$10^9\Omega$
σ	$10^{-6}\mathrm{C/m}^2$

The tested shape functions are

$$\hat{x}_{opt}=\begin{cases}0.8, & 0\le\hat{t}\le\frac{1}{6}\\ 0 & \frac{1}{6}<\hat{t}\le 1\end{cases} \tag{S72}$$

$$\hat{x}^{Har}=0.4\left(1-\cos\left(2\pi\hat{t}\right)\right) \tag{S73}$$

$$\hat{x}^{Tri}=\begin{cases}1.6\hat{t}, & 0\le\hat{t}\le\frac{1}{2}\\ 1.6-1.6\hat{t} & \frac{1}{2}<\hat{t}\le 1\end{cases} \tag{S74}$$

According to Eq.(S67) and Eq.(S71)

$$\hat{x}_{opt}^{Har}=\begin{cases}0.4\left(1-\cos\left(4.361\pi\hat{t}\right)\right), & 0\le\hat{t}\le 0.459\\ 0 & 0.459<\hat{t}\le 1\end{cases} \tag{S75}$$

$$\hat{x}_{opt}^{Tri}=\begin{cases}3.276\hat{t}, & 0\le\hat{t}\le 0.244\\ 1.6-3.276\hat{t}, & 0.244<\hat{t}\le 0.488\\ 0, & 0.488<\hat{t}\le 1\end{cases} \tag{S76}$$

SI 4.5 The tested case in Fig.4

Parameters of the tested TENG are shown in Tab.(S4)

Table S4: Parameters of the tested TENG.

Parameter	Value
L	20mm
W	20mm
d_1	0.2mm
d_2	0.2mm
ϵ_1/ϵ_0	4
ϵ_2/ϵ_0	2
R	$10^9\Omega$
σ	$10^{-6}\mathrm{C/m^2}$

The tested shape functions are

$$\hat{x}_i=\begin{cases}0.4\left(1-\cos\left(2\pi N_i\hat{t}\right)\right), & 0\le\hat{t}\le\frac{1}{N_i}\\ 0, & \frac{1}{N_i}<\hat{t}\le 1\end{cases} \tag{S77}$$

where $i=1,2,3,4,5,6$ and $N_1=1$, $N_2=2$, $N_3=3$, $N_4=4$, $N_5=6$, $N_6=12$.

SI 5 : For *Matching resistance and resonant state*

SI 5.1 Matching resistance and matching similarity number

The average power output is

$$\overline{P^S}=\frac{1}{T}\int_0^T\left(I^S\right)^2R\mathrm{d}t=\frac{\delta^2\sigma^2}{\epsilon_0^2}\frac{1}{R}\int_0^1\hat{g}^2\left(\hat{j}-\hat{Q}^S\right)^2\mathrm{d}\hat{t} \tag{S78}$$

When the resistance R equals the matching resistance R^M, we have

$$\begin{aligned}\frac{\mathrm{d}\overline{P^S}}{\mathrm{d}R}&=\frac{\delta^2\sigma^2}{\epsilon_0^2}\frac{\mathrm{d}}{\mathrm{d}R}\left(\frac{1}{R}\int_0^1\hat{g}^2\left(\hat{j}-\hat{Q}^S\right)^2\mathrm{d}\hat{t}\right)\\ &=\frac{\delta^2\sigma^2}{\epsilon_0^2}\frac{\mathrm{d}}{\mathrm{d}R}\left(\frac{1}{R}\alpha\right)=\frac{\delta^2\sigma^2}{\epsilon_0^2}\left(\frac{\mathrm{d}}{\mathrm{d}R}\left(\frac{1}{R}\right)\alpha+\frac{1}{R}\frac{\mathrm{d}\alpha}{\mathrm{d}R}\right)\\ &=\frac{\delta^2\sigma^2}{\epsilon_0^2}\left(-\frac{\alpha}{R^2}+\frac{1}{R}\frac{\mathrm{d}\alpha}{\mathrm{d}R}\right)\\ &=0\end{aligned} \tag{S79}$$

then

$$\frac{\alpha}{R} = \frac{\mathrm{d}\alpha}{\mathrm{d}R} \tag{S80}$$

where $\alpha = \int_0^1 \hat{g}^2 \left(\hat{j} - \hat{Q}^S\right)^2 \mathrm{d}\hat{t}$. Due to

$$\frac{\mathrm{d}\alpha}{\mathrm{d}R} = \frac{\mathrm{d}\alpha}{\mathrm{d}S_m}\frac{\mathrm{d}S_m}{\mathrm{d}R} = -\frac{\mathrm{d}\alpha}{\mathrm{d}S_m}\frac{S_m}{R} \tag{S81}$$

Eq.S80 can be written as

$$\alpha = -S_m \frac{\mathrm{d}\alpha}{\mathrm{d}S_m} \tag{S82}$$

that is

$$\int_0^1 \hat{g}^2 \left(\hat{j} - \hat{Q}^S\right)^2 \mathrm{d}\hat{t} = 2S_m \int_0^1 \hat{g}^2 \left(\hat{j} - \hat{Q}^S\right) \frac{\mathrm{d}\hat{Q}^S}{\mathrm{d}S_m}\mathrm{d}\hat{t} \tag{S83}$$

Notice that Eq.S83 is an equation solely in terms of S_m, and let its solution be denoted as S_m^M. Evidently, when $S_m = S_m^M$, $R = R^M$. In other words, for a specific motion input (shape function), there exists a matching similarity number S_m^M, and its corresponding resistance is the matching resistance R^M

$$R^M = \frac{\delta T}{\epsilon_0 W L S_m^M} \tag{S84}$$

SI 5.2 The tested cases in Figure.7

Table S5: The parameters in the tested cases.

Parameters	Case 1	Case 2	Case 3	Case 4
L(mm)	20	20	40	20
W(mm)	20	20	20	20
d_1(mm)	0.2	0.1	0.2	0.2
d_2(mm)	0.2	0.1	0.2	0.2
T(s)	0.5	0.5	0.5	0.3
ϵ_1/ϵ_0		4		
ϵ_2/ϵ_0		2		
σ(C/m^2)		10^{-6}		

SI 5.3 $S_m^M = 2\pi\sqrt{1-\hat{x}_m}$

In Eq.(S83)

$$\hat{Q}^S = \frac{\hat{Q}(1)}{1 - \hat{K}^{-1}(1)}\frac{1}{\hat{K}} + \hat{Q} \tag{S85}$$

$$\begin{aligned}\frac{\mathrm{d}\hat{Q}^S}{\mathrm{d}S_m} &= \frac{\mathrm{d}}{\mathrm{d}S_m}\left(\frac{\hat{Q}(1)}{1 - \hat{K}^{-1}(1)}\frac{1}{\hat{K}} + \hat{Q}\right) \\ &= \frac{\mathrm{d}}{\mathrm{d}S_m}\left(\frac{\hat{Q}(1)\hat{K}(1)}{\hat{K}(1) - 1}\right)\frac{1}{K} + \left(\frac{\hat{Q}(1)\hat{K}(1)}{\hat{K}(1) - 1}\right)\frac{\mathrm{d}}{\mathrm{d}S_m}\left(\frac{1}{K}\right) + \frac{\mathrm{d}\hat{Q}}{\mathrm{d}S_m}\end{aligned} \tag{S86}$$

where

$$\frac{\mathrm{d}\hat{K}}{\mathrm{d}S_m} = \hat{G}\hat{K} \tag{S87}$$

$$\begin{aligned}\frac{\mathrm{d}\hat{Q}}{\mathrm{d}S_m} &= \frac{\mathrm{d}}{\mathrm{d}S_m}\left(\frac{S_m}{\hat{K}}\right)\int_0^{\hat{t}}\hat{j}\hat{g}\hat{K}\mathrm{d}\hat{\xi} + \frac{S_m}{\hat{K}}\frac{\mathrm{d}}{\mathrm{d}S_m}\int_0^{\hat{t}}\hat{j}\hat{g}\hat{K}\mathrm{d}\hat{\xi} \\ &= \frac{1-S_m\hat{G}}{\hat{K}}\int_0^{\hat{t}}\hat{j}\hat{g}\hat{K}\mathrm{d}\hat{\xi} + \frac{S_m}{\hat{K}}\int_0^{\hat{t}}\hat{j}\hat{g}\hat{G}\hat{K}\mathrm{d}\hat{\xi} \\ &= \left(\frac{1}{S_m}-\hat{G}\right)\hat{Q} + \frac{1}{\hat{K}}\int_1^{\hat{K}(\hat{t})}\hat{j}\hat{G}\mathrm{d}\hat{K}\end{aligned} \tag{S88}$$

For the lateral sliding mode TENG and the harmonic shape function $\hat{x} = \frac{\hat{x}_m}{2}\left(1-\cos(2\pi\hat{t})\right)$, we have

$$\hat{j} = \hat{x} = \frac{\hat{x}_m}{2}\left(1-\cos 2\pi\hat{t}\right) \tag{S89}$$

$$\hat{g} = \frac{1}{1-\hat{x}} = \frac{1}{1-\frac{\hat{x}_m}{2}+\frac{\hat{x}_m}{2}\cos 2\pi\hat{t}} \tag{S90}$$

Notice that, at this point, $S_m = 2\pi\sqrt{1-\hat{x}_m}$ is an approximate solution to Eq.(S83), which can be proven as follows.

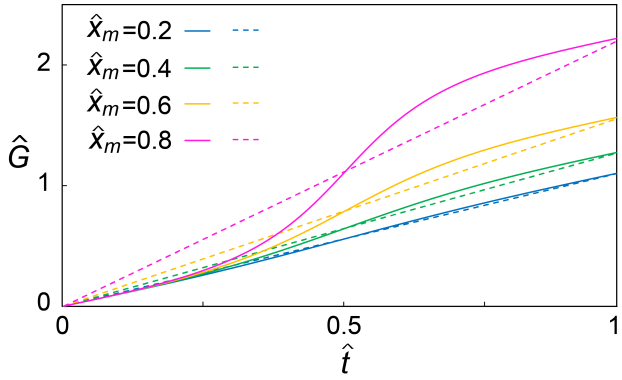

Figure S7: A comparison between function $\hat{G}$ and function $(1-\hat{x}_m)^{-1/2}\hat{t}$.

It can been seen that, as shown in Fig.(S7), when $\hat{x}_m$ is relatively small, function $\hat{G}$ approximates a linear function

$$\hat{G} \approx \frac{1}{\sqrt{1-\hat{x}_m}}\hat{t} \tag{S91}$$

If $S_m = 2\pi\sqrt{1-\hat{x}_m}$ we have

$$\hat{K} = e^{S_m\hat{G}} = e^{2\pi\hat{t}} \tag{S92}$$

$$\hat{t} = \frac{1}{2\pi}\ln\hat{K} \tag{S93}$$

Therefore

$$\hat{Q} = \frac{1}{\hat{K}}\int_1^{\hat{K}(\hat{t})}\frac{\hat{x}_m}{2}\left(1-\cos\ln\hat{K}\right)\mathrm{d}\hat{K} = \frac{\hat{x}_m}{2}\left(1-\frac{1}{2}\cos 2\pi\hat{t}-\frac{1}{2}\sin 2\pi\hat{t}-\frac{1}{2\hat{K}}\right) \tag{S94}$$

$$\hat{Q}^S = \frac{\hat{Q}(1)}{1-\hat{K}^{-1}(1)}\frac{1}{\hat{K}} + \hat{Q} = \frac{\hat{x}_m}{2}\left(1-\frac{1}{2}\cos 2\pi\hat{t}-\frac{1}{2}\sin 2\pi\hat{t}\right) \tag{S95}$$

$$\begin{aligned}\frac{\mathrm{d}\hat{Q}}{\mathrm{d}S_m} &= \left(\frac{1}{S_m}-\hat{G}\right)\hat{Q} + \frac{1}{\hat{K}}\int_1^{\hat{K}(\hat{t})}\hat{j}\hat{G}\mathrm{d}\hat{K} \\ &= \left(\frac{1}{S_m}-\hat{G}\right)\hat{Q} + \frac{1}{2\pi\sqrt{1-\hat{x}_m}}\frac{1}{\hat{K}}\int_1^{\hat{K}(\hat{t})}\frac{\hat{x}_m}{2}\left(1-\cos\ln\hat{K}\right)\ln\hat{K}\mathrm{d}\hat{K} \\ &= \frac{\hat{x}_m}{4\pi\sqrt{1-\hat{x}_m}}\left(-\frac{1}{2}\cos 2\pi\hat{t}+\frac{1}{2\hat{K}}+\pi\hat{t}\frac{1}{\hat{K}}\right)\end{aligned} \tag{S96}$$

$$\begin{aligned}\frac{\mathrm{d}\hat{Q}^S}{\mathrm{d}S_m} &= \frac{\mathrm{d}}{\mathrm{d}S_m}\left(\frac{\hat{Q}(1)\hat{K}(1)}{\hat{K}(1)-1}\frac{1}{K}\right)+\frac{\mathrm{d}\hat{Q}}{\mathrm{d}S_m}\\ &= -\frac{\omega_0}{2}\frac{1}{\hat{K}}\left(\frac{1}{S_m}+\hat{G}\right)+\left(\frac{1}{S_m}-\hat{G}\right)\hat{Q}+\frac{1}{\hat{K}}\int_1^{\hat{K}(\hat{t})}\hat{j}\hat{G}\mathrm{d}\hat{K}\\ &= -\frac{1}{4}\frac{\hat{x}_m}{S_m}\cos 2\pi\hat{t}\end{aligned} \tag{S97}$$

Considering the symmetry, the left side of Eq.S83 has

$$\int_0^1 \hat{g}^2\left(\hat{j}-\hat{Q}^S\right)^2\mathrm{d}\hat{t} = \frac{\hat{x}_m^2}{16}\int_0^1 \hat{g}^2\left(\sin 2\pi\hat{t}-\cos 2\pi\hat{t}\right)^2\mathrm{d}\hat{t} = \frac{\hat{x}_m^2}{16}\int_0^1 \hat{g}^2\mathrm{d}\hat{t} \tag{S98}$$

The right side of Eq.S83 has

$$\begin{aligned}2S_m\int_0^1 \hat{g}^2\left(\hat{j}-\hat{Q}^S\right)\frac{\mathrm{d}\hat{Q}^S}{\mathrm{d}S_m}\mathrm{d}\hat{t} &= \frac{\hat{x}_m^2}{8}\int_0^1 \hat{g}^2(\sin 2\pi\hat{t}-\cos 2\pi\hat{t})(-\cos 2\pi\hat{t})\mathrm{d}\hat{t}\\ &= \frac{\hat{x}_m^2}{8}\int_0^1 \hat{g}^2(\cos 2\pi\hat{t})^2\mathrm{d}\hat{t}\end{aligned} \tag{S99}$$

When $\hat{x}_m$ is relatively small, $\hat{g}$ doesn't change much with $\hat{t}$ and can be approximated as a constant. Consequently, the two integrals above are equal, and Eq.(S83) approximately holds.

SI 5.4 The time-average oscillation frequency of TENG system $\overline{\omega_T}$

The capacitance of TENG under the dimensionless displacement $\hat{x}$ is

$$C = \frac{\epsilon_0 WL(1-\hat{x})}{\delta} \tag{S100}$$

At this point, the angular frequency and its time-average value of the TENG system are

$$\omega_T = \frac{\delta}{\epsilon_0 WLR(1-\hat{x})} = \frac{\omega_0}{1-\hat{x}} = \hat{g}\omega_0 \tag{S101}$$

$$\overline{\omega_T} = \omega_0\int_0^1 \hat{g}\mathrm{d}\hat{t} = \omega_0\hat{G}(1) \tag{S102}$$

Shape functions in the Fig.(S8) are

$$\hat{x} = \frac{\hat{x}_m}{2}\left(1-\cos\left(2\pi\hat{t}\right)\right) \tag{S103}$$

$$\hat{x} = \begin{cases}\frac{\hat{x}_m}{2}\left(1-\cos\left(4\pi\hat{t}\right)\right), & 0\le\hat{t}\le\frac{1}{2}\\ 0, & \frac{1}{2}<\hat{t}\le 1\end{cases} \tag{S104}$$

$$\hat{x} = \begin{cases}2\hat{x}_m\hat{t}, & 0\le\hat{t}\le\frac{1}{2}\\ 2\hat{x}_m-2\hat{x}_m\hat{t}, & \frac{1}{2}<\hat{t}\le 1\end{cases} \tag{S105}$$

$$\hat{x} = \begin{cases}4\hat{x}_m\hat{t}, & 0\le\hat{t}\le\frac{1}{4}\\ 2\hat{x}_m-4\hat{x}_m\hat{t}, & \frac{1}{4}<\hat{t}\le\frac{1}{2}\\ 0, & \frac{1}{2}<\hat{t}\le 1\end{cases} \tag{S106}$$

Correspondingly, under resonance conditions, the ratios of the time-average oscillation frequency of the TENG system to the motion input frequency $\overline{\omega_T}/\omega = \hat{G}(1)\omega_0/\omega = \hat{G}(1)S_m^M/2/\pi$ are

$$\frac{\overline{\omega_T}}{\omega} = \frac{1}{2\pi}\hat{G}(1)S_m^M = \frac{1}{2\pi}\int_0^1\frac{1}{1-\frac{\hat{x}_m}{2}\left(1-\cos\left(2\pi\hat{t}\right)\right)}\mathrm{d}\hat{t}S_m^M = \frac{1}{2\pi}\frac{1}{\sqrt{1-\hat{x}_m}}S_m^M \tag{S107}$$

$$\frac{\overline{\omega_T}}{\omega}=\frac{1}{2\pi}\hat{G}(1)S_m^M=\frac{1}{2\pi}\left(\int_0^{0.5}\frac{1}{1-\frac{\hat{x}_m}{2}\left(1-\cos\left(4\pi\hat{t}\right)\right)}\mathrm{d}\hat{t}+\frac{1}{2}\right)S_m^M=\frac{1}{2\pi}\frac{1}{2}\left(\frac{1}{\sqrt{1-\hat{x}_m}}+1\right)S_m^M \tag{S108}$$

$$\frac{\overline{\omega_T}}{\omega}=\frac{1}{2\pi}\hat{G}(1)S_m^M=\frac{1}{2\pi}\left(2\int_0^{0.5}\frac{1}{1-2\hat{x}_m\hat{t}}\mathrm{d}\hat{t}\right)S_m^M=\frac{1}{2\pi}\frac{1}{\hat{x}_m}\ln\left(\frac{1}{1-\hat{x}_m}\right)S_m^M \tag{S109}$$

$$\frac{\overline{\omega_T}}{\omega}=\frac{1}{2\pi}\hat{G}(1)S_m^M=\frac{1}{2\pi}\left(2\int_0^{0.25}\frac{1}{1-4\hat{x}_m\hat{t}}\mathrm{d}\hat{t}+\frac{1}{2}\right)S_m^M=\frac{1}{2\pi}\frac{1}{2}\left(\frac{1}{\hat{x}_m}\ln\left(\frac{1}{1-\hat{x}_m}\right)+1\right)S_m^M \tag{S110}$$

where S_m^M can be obtained via numerical methods.

Parameters of the tested TENG are shown in Tab.(S6)

Table S6: Parameters of the tested TENG.

Parameter	Value
L	20mm
W	20mm
d_1	0.2mm
d_2	0.2mm
ϵ_1/ϵ_0	4
ϵ_2/ϵ_0	2
σ	10^{-6}C/m^2
T	0.5s

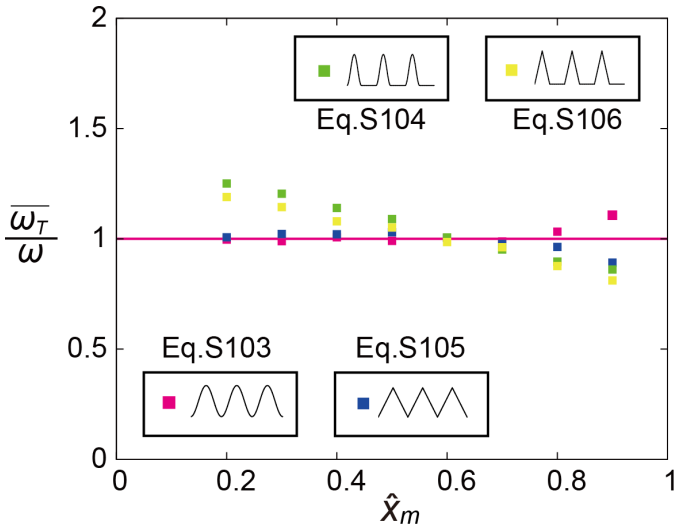

Figure S8: Resonance state.

SI 5.5 Experimental data and estimated matching resistances in Fig.5(d-f)

The experimental data presented in Figure Fig.5(d-f) were obtained from experiments on contact-separation mode TENGs, with the corresponding test parameters provided in Tab.(S7). The motion inputs employed in the experiments were simple harmonic functions with an amplitude of 1mm.

Table S7: The parameters of the TENGs in Fig.6(d-f).

	(d)	(e)	(f)
Reference	(Dharmasena et al., 2018a)	(Dharmasena et al., 2018a)	(Dharmasena et al., 2018b)
L(m)	0.05	0.05	0.05
W(m)	0.05	0.05	0.05
d_1(m)	0.00022	0.00022	0.00022
d_2(m)	0.0002	0.0002	-
T(s)	1	0.1	1
ϵ_1/ϵ_0	3.24	3.24	3.24
ϵ_2/ϵ_0	3.3	3.3	-

For the contact-separation mode TENGs, the structural characteristic relation $\hat{g}$ is (see SI 6)

$$\hat{g} = 1 + \hat{y} \tag{S111}$$

where $\hat{y} = \frac{y}{\delta}$ is the dimensionless displacement. Under a simple harmonic motion input, we have

$$\hat{G}(1) = \int_0^1 \hat{g} \mathrm{d}\hat{t} = 1 + \frac{\hat{y}_m}{2} \tag{S112}$$

where $\hat{y}_m$ denotes the maximum dimensionless displacement. Therefore, the matching resistances are respectively estimated to be

$$R^M = \frac{1}{2\pi} \frac{\delta T}{\epsilon_0 W L} \hat{G}(1) = \frac{1}{2\pi} \frac{0.000129 \times 1}{8.85 \times 10^{-12} \times 0.05 \times 0.05} \times \left(1 + \frac{0.002}{2 \times 0.000129}\right) = 8.12 \times 10^9 \Omega \tag{S113}$$

$$R^M = \frac{1}{2\pi} \frac{0.000129 \times 0.1}{8.85 \times 10^{-12} \times 0.05 \times 0.05} \times \left(1 + \frac{0.002}{2 \times 0.000129}\right) = 8.12 \times 10^8 \Omega \tag{S114}$$

$$R^M = \frac{1}{2\pi} \frac{0.0000679 \times 1}{8.85 \times 10^{-12} \times 0.05 \times 0.05} \times \left(1 + \frac{0.002}{2 \times 0.0000679}\right) = 7.68 \times 10^9 \Omega \tag{S115}$$

The experimental data and estimated values exhibit the same order of magnitude. The discrepancies are partially rooted in the parallel-plate capacitor assumption, as evidenced by the obvious divergence between the open-circuit voltage V_{OC} predicted by the classical model based on this assumption and those derived from advanced models such as the 3D model and the DDEF model(Dharmasena et al., 2018a). Herein, the DDEF model is adopted to modify the estimation formula by recalibrate the structural characteristic relationship $\hat{g}$.

$$\hat{g} = \frac{C_0}{C} = C_0 \frac{V_{OC}}{Q_{SC}} = \frac{\epsilon_0 W L}{\delta} \frac{\delta + y}{\sigma W L y} V_{OC} = \frac{\epsilon_0}{\sigma} (1 + \hat{y}) \frac{V_{OC}}{y} \tag{S116}$$

$$\hat{G}(1) = \int_0^1 \hat{g} \mathrm{d}\hat{t} = \sum \hat{g}|_{\hat{y}(\hat{t}_i)} \Delta \hat{t}_i \tag{S117}$$

The OC voltage-displacement relationship $V_{OC} - y$ can be found in references (Dharmasena et al., 2017, 2018b). The structural characteristic relationships $\hat{g} - \hat{y}$ before and after correction are presented in Fig.(S9). The corrected estimated resistance values are $2.35 \times 10^9 \Omega$, $2.35 \times 10^8 \Omega$ and $4.80 \times 10^9 \Omega$, respectively.

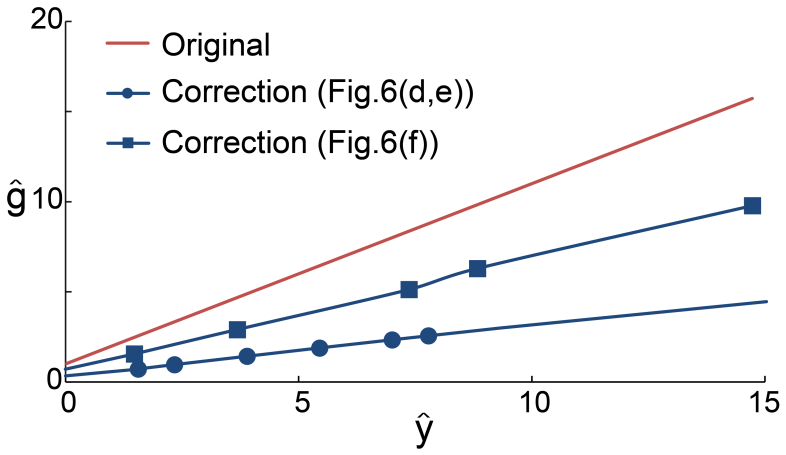

Figure S9: The structural characteristic relationships $\hat{g}-\hat{y}$ before and after correction.

SI 6 : For *Applicability*

The preceding analysis of TENG dynamics is predicated upon the following premises: (1) The characteristic frequency $\omega_0 = \delta/(\epsilon_0 WLR)$; (2) The structural characteristic relationship $\hat{g}$ exhibits monotonic increase with respect to $\hat{x}$; (3) $\hat{g}\hat{j} = \hat{g} - 1$. These premises are not exclusive to the lateral sliding mode TENG but are also prevalent in TENGs of other structures, such as the contact-separation mode and a hybrid mode.

SI 6.1 Contact-separation mode

For the contact-separation mode TENG in Fig.S10, we have

Table S8: Structural characteristic relations of the contact-separation mode TENG

Function	Expression
C	$\epsilon_0 WL/(\delta + y)$
Q_{SC}	$\sigma WLy/(\delta + y)$
ω_0	$\delta/(\epsilon_0 WLR)$
$\hat{y}$	y/δ
$\hat{g}$	$1 + \hat{y}$
$\hat{j}$	$\hat{y}/(1 + \hat{y})$

Obviously, $\hat{g}$ is monotonically increasing with respect to $\hat{x}$, and

$$\hat{g}\hat{j} = \hat{g} - 1 \tag{S118}$$

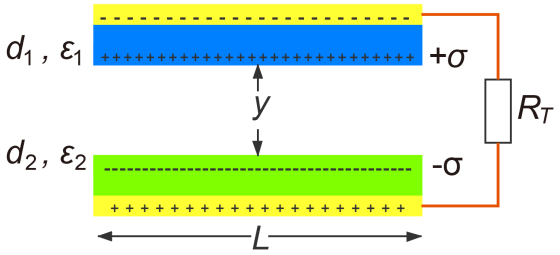

Figure S10: Contact-separation mode TENG.

SI 6.2 The hybrid mode

The TENG looks like a hybrid TENG combining lateral sliding mode and free-standing mode, with four triboelectric layers. From top to bottom, the thicknesses of the triboelectric layers are d_1, d_3, d_4 and d_2, and their respective dielectric constants are ϵ_1, ϵ_2, ϵ_1 and ϵ_2. The upper and lower dielectric layers are fixed, while the middle two layers can slide horizontally, thus generating the same charge density σ on surfaces and subsequently producing current in the external circuit.

At open-circuit condition shown in Fig.S11, assume the induced charge densities on the electrode are σ_1 and σ_2

$$\sigma_1 x = \sigma_2 (L - x) \tag{S119}$$

As the electrode is equipotential, it implies that

$$V_{OC} = \frac{\sigma}{\epsilon_0}(d_3 + d_4) - \frac{\sigma_1}{\epsilon_0}(\delta_1 + d_3 + d_4) = \frac{\sigma_2}{\epsilon_0}\delta \tag{S120}$$

where

$$\delta = \epsilon_0 \left(\frac{d_1 + d_4}{\epsilon_1} + \frac{d_2 + d_3}{\epsilon_2} \right) \tag{S121}$$

$$\delta_1 = \epsilon_0 \left(\frac{d_1}{\epsilon_1} + \frac{d_2}{\epsilon_2} \right) \tag{S122}$$

Then, we get

$$V_{OC} = \frac{\sigma\delta}{\epsilon_0} \frac{d_3 + d_4}{\delta - (\delta_1 + d_3 + d_4) + \frac{L}{x}(\delta_1 + d_3 + d_4)} \tag{S123}$$

At short-circuit condition shown in Fig.S12, assume the induced charge density on the electrode is σ_3

$$\frac{\sigma}{\epsilon_0}(d_3 + d_4) = \frac{\sigma_3}{\epsilon_0}(\delta_1 + d_3 + d_4) \tag{S124}$$

Then

$$Q_{SC} = \sigma_3 x W = \sigma x W B_1 = \sigma x W \frac{d_3 + d_4}{\delta_1 + d_3 + d_4} \tag{S125}$$

Combining Eq.(S123) and Eq.(S125), we get

$$C = \frac{Q_{SC}}{V_{OC}} = \frac{\epsilon_0}{\delta} W L \left(1 - B_2 \frac{x}{L}\right) = \frac{\epsilon_0}{\delta} W L \left(1 - \frac{\delta_1 + d_3 + d_4 - \delta}{\delta_1 + d_3 + d_4} \frac{x}{L}\right) \tag{S126}$$

Let

$$\omega_0 = \frac{\delta}{\epsilon_0 W L R} \tag{S127}$$

Then

$$\hat{j} = \frac{Q_{SC}}{q} = l_1 \hat{x} \tag{S128}$$

$$\hat{g} = \frac{1}{\omega_0 R_T C} = \frac{1}{1 - l_2 \hat{x}} \tag{S129}$$

Therefore

$$\hat{g}\hat{j} = l(\hat{g} - 1) = \frac{l_1}{l_2}(\hat{g} - 1) = \frac{d_3 + d_4}{\left(1 - \frac{\epsilon_0}{\epsilon_2}\right) d_3 + \left(1 - \frac{\epsilon_0}{\epsilon_1}\right) d_4}(\hat{g} - 1) \tag{S130}$$

This equation, although it contains an additional coefficient l compared to premise 3, is equally applicable to the aforementioned analysis.

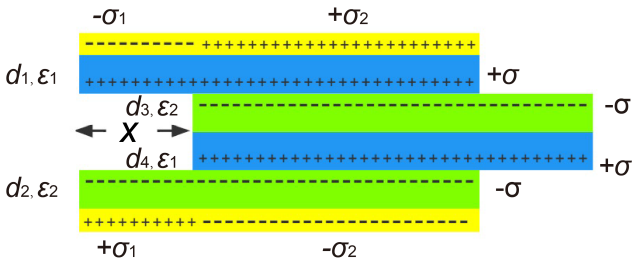

Figure S11: Open-circuit condition.

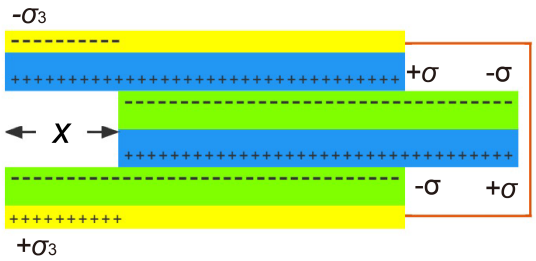

Figure S12: Short-circuit condition.

References

Dharmasena RDIG, Deane JHB, Silva SRP. Nature of power generation and output optimization criteria for triboelectric nanogenerators. ADVANCED ENERGY MATERIALS 2018a;8(31).

Dharmasena RDIG, Jayawardena KDGI, Mills CA, Dorey RA, Silva SRP. A unified theoretical model for triboelectric nanogenerators. NANO ENERGY 2018b;48:391–400.

Dharmasena RDIG, Jayawardena KDGI, Mills CA, Deane JHB, Anguita JV, Dorey RA, et al. Triboelectric nanogenerators: providing a fundamental framework. ENERGY & ENVIRONMENTAL SCIENCE 2017;10(8):1801–11.